Hindawi
International Journal of Aerospace Engineering
Volume 2018, Article ID 8759836, 9 pages
https://doi.org/10.1155/2018/8759836

Research Article

UAV Path Prediction for CD&R to Manned Aircraft in a Confined Airspace for Cooperative Mission

Chin E. Lin and Ya-Hsien Lai

Department of Aeronautics and Astronautics, National Cheng Kung University, Tainan 701, Taiwan

Correspondence should be addressed to Chin E. Lin; chinelin@mail.ncku.edu.tw

Received 15 June 2017; Revised 26 November 2017; Accepted 28 November 2017; Published 1 March 2018

Academic Editor: Angel Velazquez

In this paper, a new path prediction approach for unmanned aerial vehicles (UAVs) for conflict detection and resolution (CD&R) to manned aircraft in cooperative mission in a confined airspace is proposed. Path prediction algorithm is established to estimate UAV flight trajectory to predict conflict threat to manned aircraft in time advances (front-end process of CD&R system). A hybrid fusion model is formulated based on three different trajectory prediction conditions considering scenarios in geographical conditions to aid the generation of appropriate resolution advisory of conflict alert. It offers a more precise CD&R system for manned and unmanned aircraft in cooperative rescue missions.

1. Introduction

As time progresses, the use of unmanned aerial vehicles (UAVs) dramatically increases. Missions are flown for all usages such as surveillance, research, agricultural, and disaster. These missions are carried out mostly with only UAVs in the airspace due to its straightforward mission plans. But with the focus of this study in disaster site which includes search and rescue missions in a confined airspace, cooperative missions between manned and unmanned aerial vehicles are inevitable. In low-altitude flights, the traditional surveillance methods are not effective. In NextGen development concept, detect and avoid (DAA) mechanism may also not be efficient either [1]. This factor brings a big risk for manned aircraft safety in cooperative flights.

CD&R systems are equipped onto the aircraft to ensure flight safety. Commercial manned aircraft are equipped with TCAS [2], while other algorithms for manned aircraft CD&R systems have been proposed and verified with positive results [3]. In recent decade, different unmanned CD&R designs have also been developed to adopt different situations [4]. Although many CD&R studies show promising results, the basic front-end processing assumptions of the studies do not relate to the real-world confined airspace environment for this study.

This paper will focus on proposing a more realistic path-predicting method to correspond to the confined airspace environment parameters. The confined airspace assumption in this research is to simulate an airspace around a disaster site where multiple aerial supports are needed. The radius of the airspace is assumed to be approximately 5 km. This radius is a reasonable assumption that could cover all the land disaster sites. Due to this airspace sizing consideration and disaster site surveillance tasks, frequent flight course changes are needed.

2. Path Prediction Models

Path prediction is the very first step to CD&R systems. It is the base prediction layer with conflict detection and resolution prediction layer to complete the system. A precise prediction can reduce the false error of the CD&R system. Even with a high-performance CD&R system, an inaccurate prediction can mislead the system to generate false conflicts and resolutions.

In most CD&R researches, the focus of the research is based on the latter conflict detection and resolution layers. The front stage path prediction is often assumed to be traveling in a constant velocity and heading [5–7] or linear travels from point A to point B [8]. Some study considers free flight

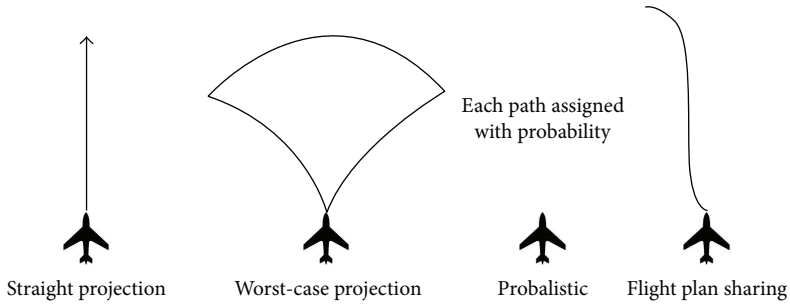

Figure 1: Schematics of path prediction models.

but still assumes only straight flight possibility [9]. These concepts are acceptable when the flight environment is an open airspace with seldom heading changes. The environment parameter in this research is focused in a confined airspace, where disaster area is cooperatively rescued. The assumptions made by those researches [5–9] cannot be adopted. A new design toward path prediction in a confined airspace will be the main interest in this paper.

Figure 1 shows the schematics of the basic path prediction models. Each model corresponds to certain flight path prediction conditions. The straight projection model is a relatively simple concept to adopt since it predicts the aircraft travel in a straight line. It is feasible if the aircraft is in a cross-country flight with little heading change and is the most adopted path prediction model due to its simplicity [10].

The worst-case projection model is the extreme of the dynamic modeling. It is a sector projection to cover all possible maneuverings by aircraft [11]. Because of the broad area of estimation, it is an ideal choice when the aircraft is operated under visual flight rule (VFR) in a confined airspace with numerous turning maneuvers being performed.

The probabilistic projection model describes the potential variations in the advanced trajectories [12]. There are mainly two ways to run. The first approach gives weights to straight projection and worst-case projection by the current states of the model. The second approach is to weight possible future estimated flight trajectories.

Flight plan sharing is a model in which each aircraft shares its planned flight path. With the abundant knowledge of each aircraft in the vicinity, a more precise prediction can be widely made [13].

The main assumption in this paper differs from other studies by assuming the aircraft having a high tendency to perform heading changes. This is due to the difference in airspace environment parameters. With this assumption as the initial parameters, linear nominal flight prediction from point to point cannot be realistic.

In this research, the only data acquired from the hardware sensors is the GPS data by automatic dependent surveillance-rebroadcast (ADS-R) mechanism [14, 15] as shown in Figure 2. Because of the minimum amount of low-altitude surveillance information can be received via ADS-R and the consistent turning maneuvers of the formulation conditions, a combination of worst-case projection, probabilistic models, and flight plan sharing is used to

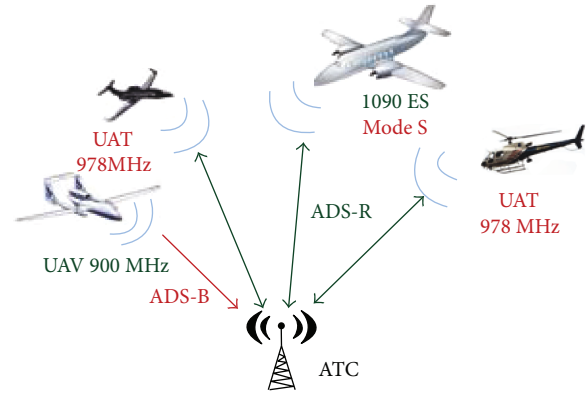

Figure 2: ADS-R for broad surveillance application.

accurately predict the advanced positions of the aircraft. These models in combination together with a hybrid system are used for manned and unmanned path prediction model, especially the UAVs.

The hybrid path prediction model is a fusion of short-/long-term estimation path planned/free flight estimation. The short-term estimation is applied for advanced prediction within 25 seconds, which meets the resolution advisory (RA) in TCAS [14]. It adopts the worst-case projection and probabilistic model as an extension from our previous research [16]. It will be equipped on all manned and unmanned aircraft in the area under ADS-R mechanism.

Nonpath planned aircraft, usually free flight manned aircraft, can only adopt the short-term sector (STS) estimation due to its high-dynamic uncertainty. Path planned aircraft, directly proposed for manned aircraft and UAVs, adopts the short-term parameter guided (STPG) estimation with correction parameters.

Environment effects such as winds are unpredictable and collectable in real time by the ground sensor detections. They are strong factors that the aircraft will need in deciding how to operate. Only introducing past data into current algorithms, the current environmental factors can be reduced into a minimum. Those correcting parameters are implanted into the STPG algorithms to further improve its accuracy in estimation.

The long-term parameter guided (LTPG) estimation is a projection of the aircraft into the future of over 1 minute. This is based on flight plan sharing and probabilistic

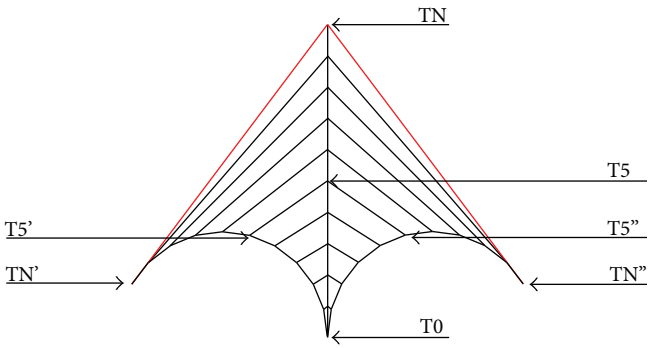

Figure 3: STS schematics.

model, which is used mainly on the UAVs or any manned aircraft with a specific flight plan. This model is used for manned aircraft to design an advanced flight plan to avoid possible conflicts.

Each aircraft adopts one of the models explained above. The different models from the aircraft are fusion together to generate a conflict area. This conflict area can be further used for conflict resolution algorithms; because conflict resolution is not in this scope of research, it will not be further explained in this paper. The STS, STPG, and LTPG models and correcting parameters will be introduced in the next section.

3. STS and STPG Models

3.1. Short-Term Sector (STS) Path Prediction Model. The short-term sector (STS) path prediction model is adopted into aircraft mainly without a precise planned path or any specific waypoints are used. This model is based on the sector CD&R system from our previous research [16]. In that research, the algorithm constructs one sector to represent the possible flight path of the aircraft for the next 25 seconds. This sector is divided into two zones, traffic advisory (TA) and resolution advisory (RA) zones [14]. By the ownership/intruder sector overlapping area percentage, different levels of warning are issued. The advantage of this concept is adopting its relatively simple in fast calculation.

But because the single sector (two zones) has to cover all 25 seconds of estimation, precise conflict area and time are relatively hard to estimate. The STS path prediction model improves the prediction by introducing time stamps into the prediction sector.

The STS model is shown in Figure 3. The top inverted V (^) is a simplification of a semicircular to increase calculation performance. It symbols the maximum distance of an aircraft traveling at constant initial velocity. The bottom hemisphere confines the aircraft's prediction model by the maximum heading change ($\psi_{\max\_d}$) of the aircraft. It represents the maximum distance the aircraft can detour from the center line with the maximum bank angle in each time stamp. ψ_d is a combination of velocity and banking angle.

$$\psi_d = \frac{90g \tan\theta}{v\pi}. \quad (1)$$

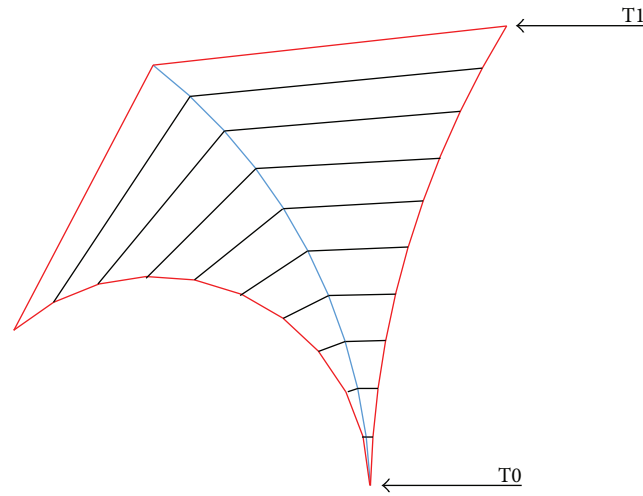

Figure 4: STS schematics with turning mechanism.

In the STS path prediction model, each second generates one sector figure to represent the estimation of the aircraft at that particular second. There are N sets of time-stamped zones (^) in each second, each representing the forward prediction zone. T0 is the current position and T1~TN is the center prediction of each future time stamp zones. T1'~TN and T1"~TN" are the leftmost and rightmost boundaries of the prediction in each zones. The center line (T0-TN) is extrapolation from the past GPS coordinates of the aircraft.

The center line takes the current (X_0, Y_0) and past two seconds (X_{-1}, Y_{-1}) and (X_{-2}, Y_{-2}) of GPS coordinates as a parameter reference.

A turning mechanism is designed to detect if the aircraft is performing a banking turn. When the heading angle differential crosses a threshold, the turning mechanism performs heading adjustments to the center line to compensate for the banking turn. The threshold can be set manually from parameters from that specific aircraft. Figure 4 shows an example of STS when the turning mechanism is active.

3.2. Short-Term Parameter Guided (STPG) Path Prediction Model. Short-term parameter guided (STPG) path prediction model uses the parameter from the flight plan and past flight data to aid the short-term prediction model. It is a hybrid model of probabilistic and flight plan sharing model. The flight path estimation is constructed based on the current coordinates and future waypoints of the aircraft. After preliminary estimation being made, correction estimations are suggested from past data. The prediction correction algorithm will be introduced in the latter section.

The preliminary predictions are made by simulating the aircraft advanced flight trajectory based on UAV flight path following the proposed algorithms. UAV uses a variety of algorithm to implement independent autopilot control and navigate itself via the designated waypoints such as carrot-chasing [17], NLGL [18], VF [19], LQR [20], and PLOS [21] with path following algorithm. One of the widely used algorithms is the carrot-chasing algorithm [17]. Although this algorithm is not suggested as the best path following

algorithm in [22], it is a simple and robust algorithm which is used on real autopilot hardware.

The carrot-chasing algorithm introduces a virtual target point (VTP), which is also called the carrot, on the path and directs the UAV to chase the VTP, until a desired path has been reached. As the engagement progresses, the UAV approaches toward the flight path and eventually follows the defined trajectory. This algorithm proposes two models describing the straight line and loiter following model.

Figure 5 is the schematics of the straight line method. The straight line method follows a straight line constructed from the past waypoint to the current waypoint ($W_i \rightarrow W_{i+1}$). On the straight line, a VTP (S) is set for the UAV to follow. The distance from the UAV to the straight line is the crosstrack error (d). The main objective is to reduce d to zero. As d decreases, the aircraft decreases the distance from the straight line and hence successfully follows the line.

In Figure 6 of the loiter mode, the UAV's task navigates around a circle O with a radius of r. To achieve the loiter, the UAV must be located on the circle and its heading direction must be orthogonal to line $\overline{Oq}$. The main objective also reduces d to zero. Both algorithms are shown below.

In both the straight line model and the loiter model, STPG path prediction model can be affected by the VTP, flight gain parameters, airspeed, and maximum banking angle of the UAV. By adjusting these parameters, an optimal trajectory can be estimated.

3.3. Prediction Correction Model. Because of minimum sensor data usage in this research (only GPS), the crosswind and other external noise acting on the aircraft cannot be detected. Assuming each aircraft characteristic is unique, the behavior of each aircraft in a single mission or environment is relatively similar. Past flight logs can be used to better estimate the flight performance of an aircraft.

After the preliminary estimations being calculated, the prediction correction algorithm is implanted. The approach in this algorithm uses the relationship of the past estimation and past flight log to assist aid to the current estimations. The correction parameters are a combination of past estimation data and past real flight data. The prediction correction algorithm is designed to use this similarity to decrease the external noise and improve estimation accuracy.

The preliminary estimation is expressed by a set of (H_i) of $25(x_i, y_i)$ coordinates. These estimation coordinates can be compared with the past sets of estimation to find the highest covariance set $(H_{\max})$. The time stamp (T_s) of the set $(H_{\max})$ can extract the specific realistic flight log (H_l) from $(T_s \sim T_{s+24})$. The distance (D) of (H_i) and (H_l) is also taken into measure as the weight of correction estimation(H_c). The algorithm is shown below in Algorithm 2. μ is the prediction correction gain.

3.4. Long-Term Parameter Guided (LTPG) Path Prediction Model. LTPG path prediction model is used on aircraft with specific flight plans defined by waypoints. With a flight plan, full flight trajectory can be mapped to ensure no conflict will occur along its trajectory. Manned aircraft can properly design preflight plans with the knowledge of the intruder LTPG model to avoid conflicts.

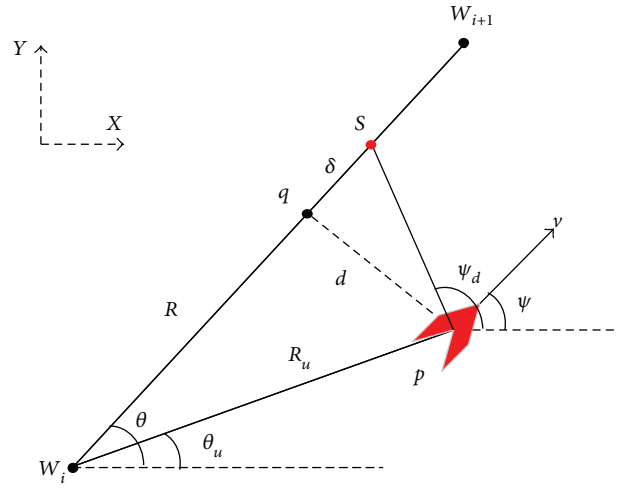

Figure 5: Straight line carrot-chasing schematics.

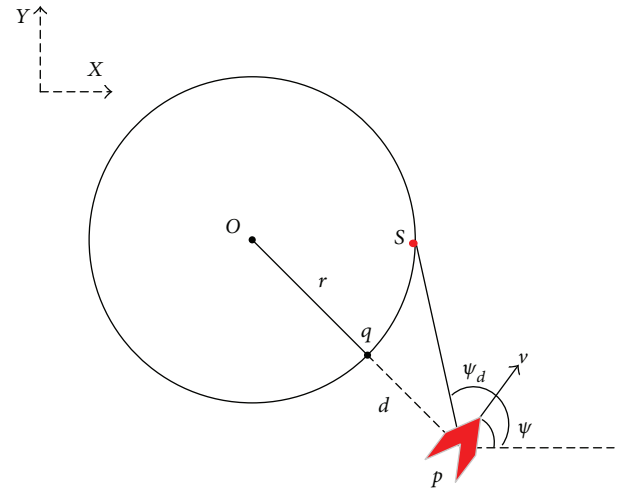

Figure 6: Loiter carrot-chasing schematics.

This model is similar with STPG path prediction model with introducing carrot-chasing algorithm as the base of the model. With all the waypoints known from the flight plan, a full trajectory can be estimated.

LTPG path prediction's main parameters are forward prediction distance (δ), flight velocity (v), maximum turning rate ($\theta_{\max}$), and flight gain (k). All these parameters affect the performance of the prediction. By adjusting these parameters, a closer prediction to the real-world trajectory can be made.

The LTPG model will not be an online conflict detection usage for pilots due to its high diverse ratio of prediction basics, but it will be an index of reference for the pilots to consider when planning preflight plans. The LTPG prediction will generate a no flight pathway which aircraft can plan ahead to avoid.

Straight line following
(1) Initialize $W_i = (x_i, y_i)$, $W_{i+1} = (x_{i+1}, y_{i+1})$, p $= (x, y)$, ψ.
(2) Calculate $s = (x_t', y_t')$,
$R_u = \|W_i - p\|$,
$\theta = \tan^{-1}(y_{i+1} - y_i, x_{i+1} - x_i)$,
$\theta_u = \tan^{-1}(y - y_i, x - x_i)$,
$\beta = \theta - \theta_u$,
$R = \sqrt{R_u^2 - (R_u \sin\beta)^2}$,
$s = (x_t', y_t') \leftarrow ((R + \delta)\cos\theta, (R + \delta)\sin\theta)$.
(3) Calculate $\psi_d = \tan^{-1}(y_t' - y, x_t' - x)$.
(4) Set control gain k.
(5) Calculate $u = \mathrm{k}(\psi_d - \psi)$.
Loiter following
(1) Initialize $O = (x_l, y_l)$, $r, p = (x, y)$, ψ.
(2) Calculate $s = (x_t', y_t')$,
$\theta = \tan^{-1}(y - y_l, x - x_l)$,
$s = (x_t', y_t') \leftarrow (r\cos(\theta + \lambda), r\sin(\theta + \lambda))$.
(3) Calculate $\psi_d = \tan^{-1}(y_t' - y, x_t' - x)$.
(4) Set control gain k.
(5) Calculate $u = k(\psi_d - \psi)$.

Algorithm 1

Prediction correction algorithm
(1) Initialize (x_i, y_i), (x_l, y_l), (x, y).
(2) Calculate $\mathrm{cov}(H_i, H)$ for all i.
(3) Find the corresponding (x_l, y_l) to the max covariance value in step 2.
(4) $D = \sqrt{(x_i - x)^2 + (y_i - y)^2}$.
(5) $(x_c, y_c) = D \times \mu \times (\mathrm{cov}(x_i, y_i) \times (x_l, y_l) + (x_i, y_i)) = (H_c)$.

Algorithm 2

Long-term parameter path prediction algorithm
(1) Initialize $\mathrm{wp}_n(x_n, y_n)$ for $n = 1 \sim$ the number of wp.
(2) Calculate prediction by algorithm 1 from $\mathrm{wp}_1 \sim \mathrm{wp}_n$.
(3) Adjust parameters from prediction to reduce real flight/prediction errors.

Algorithm 3

3.5. Parameter Training. Flight paths from the same aircraft can be used to train each model. By tuning gain values of each model, a more accurate estimation can be made by each model when operating in a real-time scenario.

4. Simulation

Actual flight data records from a self-designed CD&R system [23] are used to simulate realistic flights with turns, winds, and environment disturbances. Those data are inserted into the system in one-second intervals. In each interval, the ownership aircraft will receive its own data and intruder's data. By this way, a realistic simulation of online CD&R can be achieved.

Figure 7 is the actual recording of an UAV flight trajectory in Southern Taiwan airspace, the red circles indicate the waypoint the UAV is subjected to follow, and the blue dots are the GPS flight logs with an interval of 1 second. The total 2200 seconds of flight time is completely recorded.

Figure 8 is the manned aircraft actual flight recording. It is also a one-second interval data points but because of free flight, no waypoints are recorded. The total flight time is recorded in 1400 seconds.

The simulation is broken down into individual algorithm to better express prediction results.

4.1. STS Model. The STS model adopted on the manned aircraft flight log in Figure 8 with the comparison of the worst-

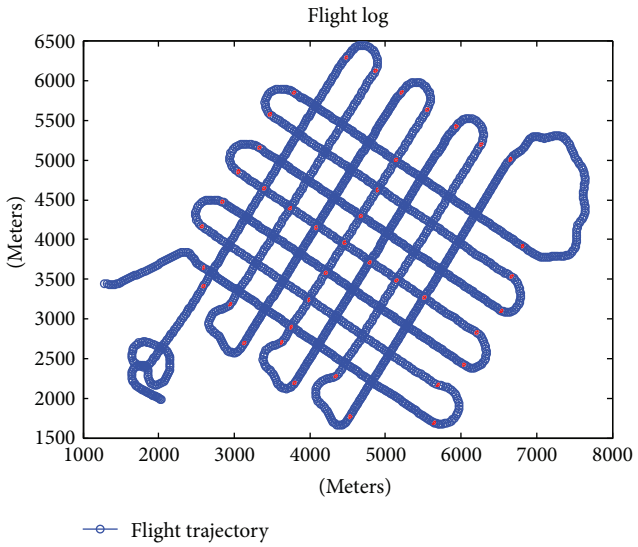

Figure 7: Flight test log of UAV.

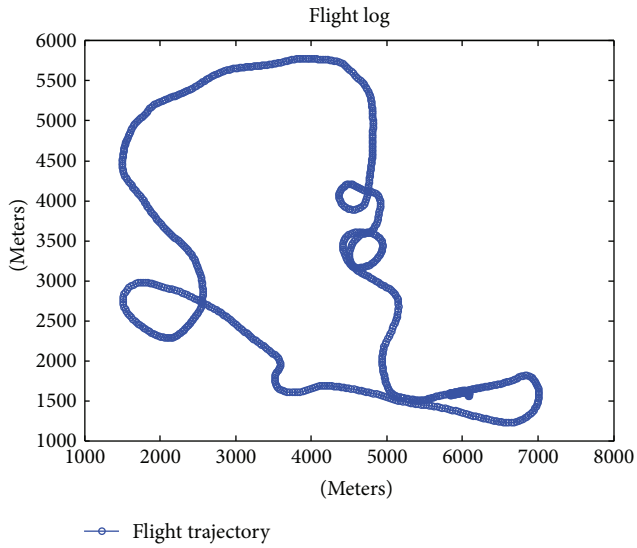

Figure 8: Flight test log of manned helicopter.

case projection (WCP) method. Figure 9 is an estimation plot at 921 seconds of the manned aircraft flight log. The solid blue lines with * symbols are the real flight trajectory. The three curved estimation lines to the right are the STS prediction with center, right, and left boundaries. These three straight estimations are the WCP estimation method. (Three lines were used to express the STS model for clearer view for comparison.)

Figure 9 is especially selected to show the difference of estimation at banking turns. From the figure, we can see STS estimation with additional curving parameters decreases the estimation errors in dramatic turn.

Figure 10 shows the average errors per second of estimation. Because the STS model is designed for forward estimation of 25 seconds, the worst-case propagation method is also calculated with forward estimation of 25 seconds. In Figure 10, the STS model errors are lower than the worst-case projection method in each second and up to 30 meters at the 25-second point, a maximum of 9.89% increase in accuracy at the 25-second point.

Figure 10 shows the prediction errors for the whole flight, but the main subject of interest in this paper is predications in turning phase of the aircraft. Figure 11 shows the prediction errors of the aircraft only when its performing bank turns. From Figure 11, it is shown although the errors of both methods increases, the error difference increases to 36%. This means the prediction of STS when turning out scales the traditional WCP prediction. The standard deviation of the errors in these predictions is shown in Figure 12. It shows that the STS model has a more condense prediction modal than the WCP model, hence giving it a more reliable prediction.

4.2. STPG Model. The STPG model is tested with the UAV flight log, because of the waypoints needed as a parameter in the STPG model. The manned flight log, as shown in Figure 8, cannot be implanted. Figure 13 shows an instance of the flight trajectory estimation with the comparison of

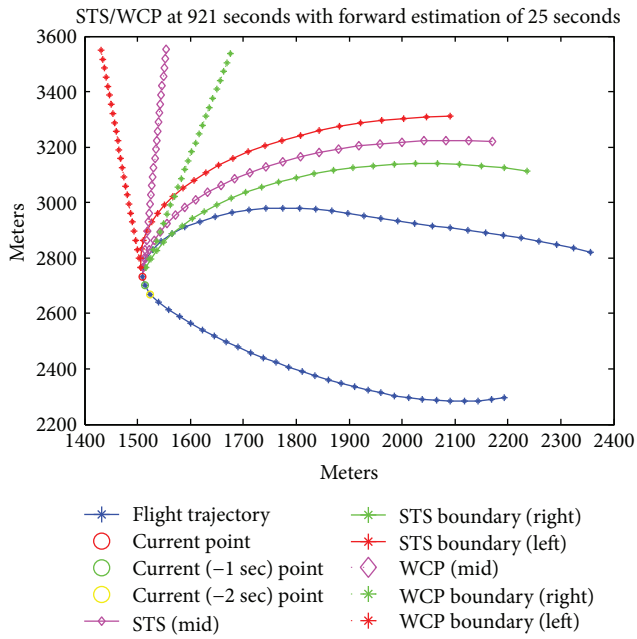

Figure 9: STS versus WCP flight estimation at 921 seconds.

STPG, STS, and WCP models. The STS shows three dashed lines at the middle, right, and left boundaries. The WCP shows dotted lines at the middle, right, and left boundaries. The STPG model is the black dot-dashed line. From Figure 13 for UAV flight log, it can clearly be shown with the aid of waypoint parameters; STPG model prediction is more accurate than both STS and WCP.

Figure 14 shows the average errors of all the models when they are implanted into the UAV flight log. The STS and WCP errors are similar to the manned aircraft flight log test in Figure 8, and there is 10.5% increase in accuracy at forward estimation of 25 seconds. The prediction errors of the STPG is slightly larger than both STS and NTP at close

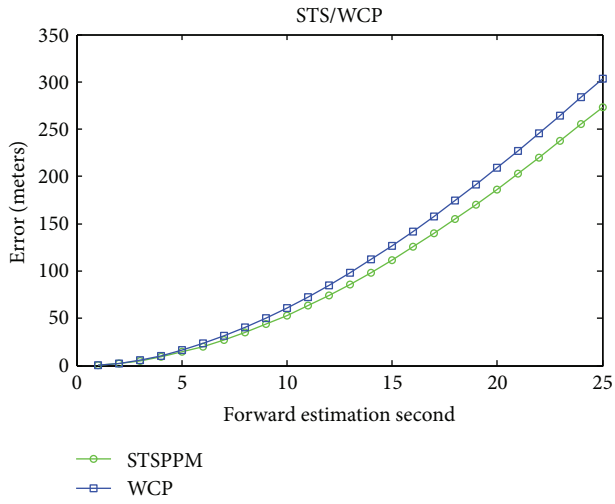

Figure 10: STS versus WCP prediction errors.

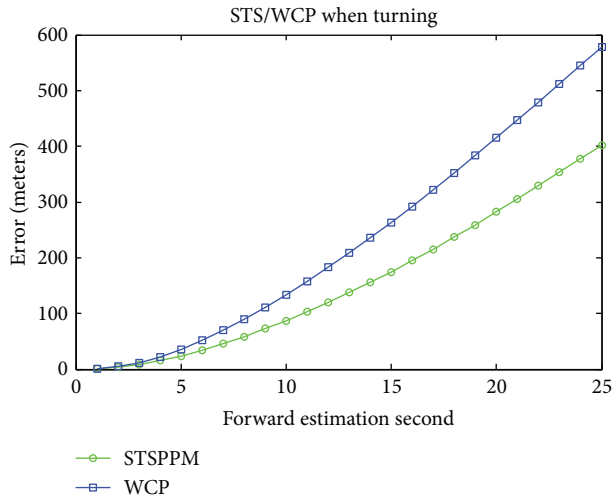

Figure 11: STS versus WCP prediction errors when turning.

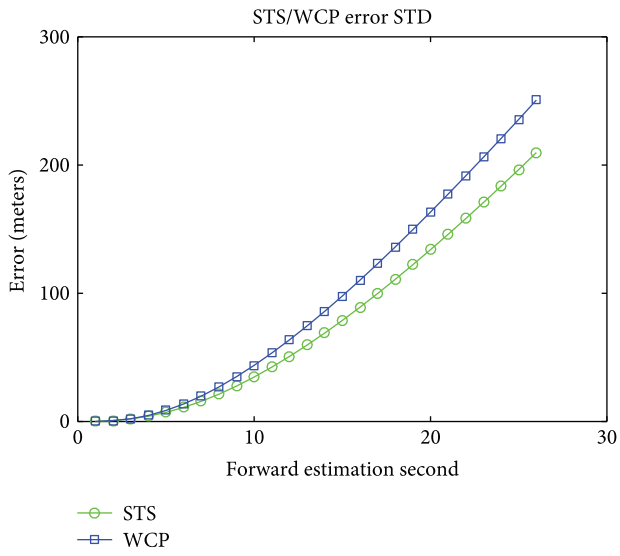

Figure 12: STS versus WCP prediction STD.

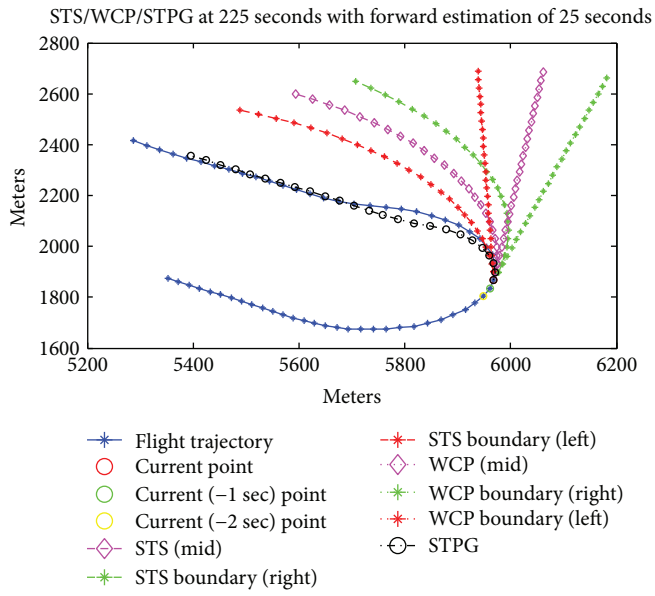

Figure 13: STPG versus STS versus WCP flight estimation at 225 seconds for UAV flight log.

forward estimation due to this average prediction error plot including straight and turns. The error of STPG is greatly reduced as prediction progresses. At the second 25 point, the accuracy has increased 62.39% against STS, and 66.36% against WCP.

Figure 15 shows the errors of prediction when the aircraft is performing banking turn. The error differences between STPG to WCP and STS are increased. The STPG accuracy is increased to 83.1% and 88.71%. This increase is due to the STPG model additional parameter assistance performance most significant at turning points. Figure 16 shows the standard deviation of all three models. STPG with its parameter prediction aids greatly improve its reliability and provides a better prediction among the others.

5. Conclusion

In this paper, a new approach towards CD&R system for bounded airspace is proposed. Because of the bounded airspace characteristics, the traditional path prediction model adopted for most CD&R model research cannot accurately predict the future coordinates of itself or intruders. Even with a good resolution model, a bad coordinate prediction can cause false judgement and false detections.

By implanting turning mechanism and waypoint parameter into STS/STPG models, a more accurate trajectory is predicted. From the above simulations, by additional turning parameters, the STS model can decrease prediction errors by 10%. When the waypoint parameters are added into the STPG model, the prediction errors decreased dramatically.

By adapting the STS/STPG model into the CD&R system, a more effective CD&R system can be designed for bounded and limited airspace.

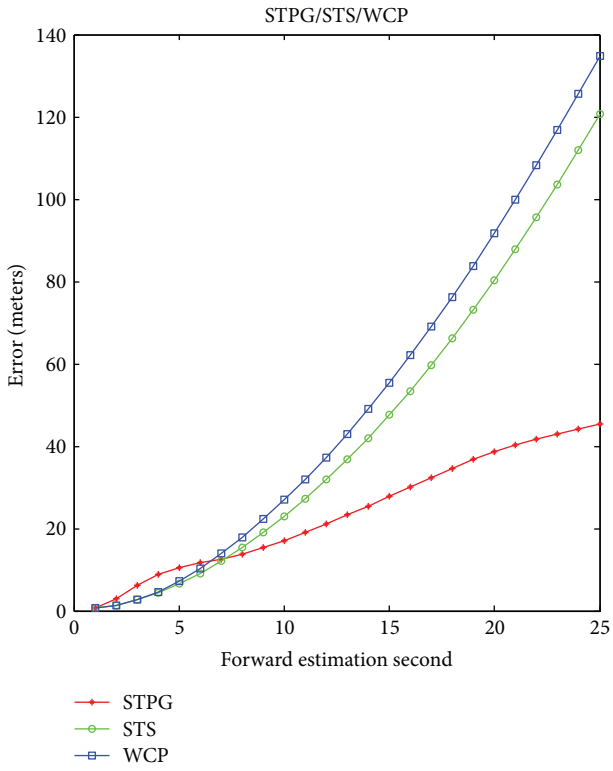

Figure 14: STS versus WCP versus STPG prediction errors.

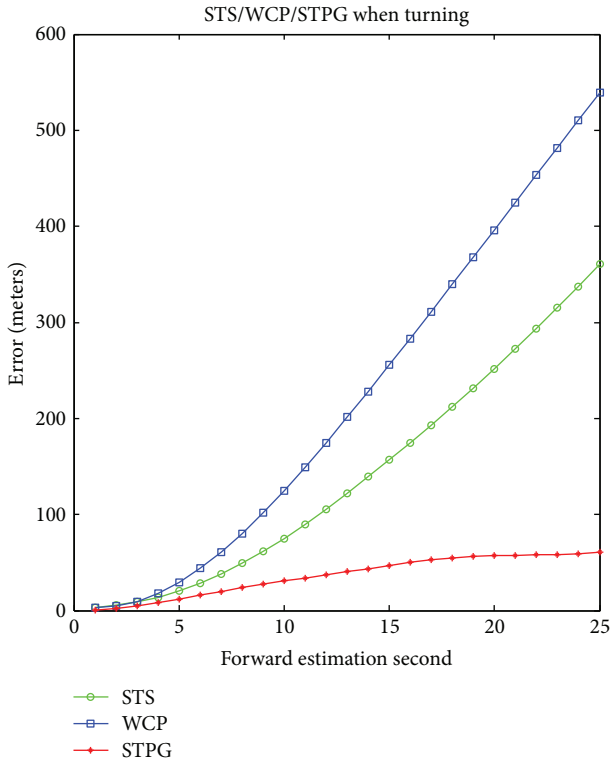

Figure 15: STS versus WCP versus STPG prediction errors when turning.

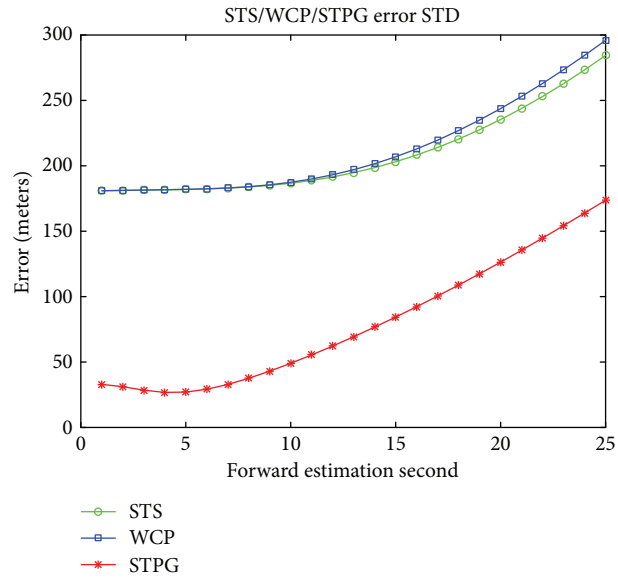

Figure 16: STS versus WCP versus STPG error STD.

Abbreviations

S: Carrot (virtual target point)
δ: Distance from VTP to q
q: Closest point from waypoint trajectory to aircraft
P: Current position
d: Cross-track error
W_i: Past waypoint
W_{i+1}: Future waypoint
V: UAV airspeed
ψ: UAV heading
ψ_d: UAV desired heading
θ: Banking angle.

Conflicts of Interest

The authors declare that there is no conflict of interest regarding the publication of this paper.

Acknowledgments

This study is supported from Ministry of Science and Technology, under Contract NSC102-2221-E-006-081-MY3.

References

[1] Federal Aviation Administration, *NextGen Implementation Plan*, US Department of Transportation, 2013.

[2] L. Peng and Y. Lin, "Study on the model for horizontal escape maneuvers in TCAS," *IEEE Transactions on Intelligent Transportation Systems*, vol. 11, no. 2, pp. 392–398, 2010.

[3] J. Kuchar and L. C. Yang, "A review of conflict detection and resolution modeling methods," *IEEE Transactions on Intelligent Transportation Systems*, vol. 1, no. 4, pp. 179–189, 2000.

[4] Y. I. Jenie, E. J. Kampen, J. Ellerbroek, and J. M. Hoekstra, "Taxonomy of conflict detection and resolution approaches for unmanned aerial vehicle in an integrated airspace," *IEEE*

Transactions on Intelligent Transportation Systems, vol. 18, no. 3, pp. 558–567, 2017.

[5] Z. H. Mao, E. Feron, and K. D. Bilimoria, "Stability and performance of intersecting aircraft flows under decentralized conflict avoidance rules," *IEEE Transactions on Intelligent Transportation Systems*, vol. 2, no. 2, pp. 101–109, 2001.

[6] J. W. Park, H. D. Oh, and M. J. Tahk, "UAV collision avoidance based on geometric approach," in *2008 SICE Annual Conference*, pp. 2122–2126, Tokyo, Japan, 2008.

[7] G. Fasano, D. Accardo, A. Moccia et al., "Multi-sensor-based fully autonomous non-cooperative collision avoidance system for unmanned air vehicles," *Journal of Aerospace Computer Information and Communication*, vol. 5, no. 10, pp. 338–360, 2008.

[8] A. Richards and J. How, "Decentralized model predictive control of cooperating UAVs," in *2004 43rd IEEE Conference on Decision and Control (CDC) (IEEE Cat. No.04CH37601)*, vol. 4, pp. 4286–4291, Nassau, Bahamas, 2004.

[9] M. Christodoulou and S. Kodaxakis, "Automatic commercial aircraft collision avoidance in free flight: the three-dimensional problem," *IEEE Transactions on Intelligent Transportation Systems*, vol. 7, no. 2, pp. 242–249, 2006.

[10] R. A. Paielli and H. Erzberger, "Conflict probability estimation for free flight," *Journal of Guidance, Control and Dynamics*, vol. 20, no. 3, pp. 588–596, 1997.

[11] K. D. Bilimoria, H. Q. Lee, Z. H. Mao, and E. Feron, "Comparison of centralized and decentralized conflict resolution strategies for multiple-aircraft problems," in *18th Applied Aerodynamics Conference*, Denver, CO, USA, August 2000.

[12] M. Innocenti, P. Gelosi, and L. Pollini, "Air traffic management using probability function fields," in *Guidance, Navigation, and Control Conference and Exhibit*, pp. 1088–1097, Portland, OR, USA, August 1999.

[13] Federal Aviation Administration, *TCAS II V7.1 Introduction*, U.S. Dept. of Transportation, 2011.

[14] C. E. Lin and C. J. Lee, "ADS-R conflict detection and resolution algorithm for general aviation in low altitude flights," *Journal of Aeronautics, Astronautics and Aviation*, vol. 48, no. 2, pp. 111–122, 2015.

[15] J. Kuchar and L. C. Yang, "Survey of conflict detection and resolution modeling methods," in *Guidance, Navigation, and Control Conference*, pp. 1388–1397, August 1997.

[16] C. E. Lin, Y. H. Lai, and F. J. Lee, "UAV collision avoidance using sector recognition in cooperative mission to helicopters," in *2014 Integrated Communications, Navigation and Surveillance Conference (ICNS) Conference Proceedings*, pp. F1-1–F1-9, Herndon, VA, USA, April 2014.

[17] G. Conte, S. Duranti, and T. Merz, "Dynamic 3D path following for an autonomous helicopter," in *Proceedings of the 5th IFAC Symposium on Intelligent Autonomous Vehicles*, pp. 473–478, Oxford, UK, 2004.

[18] S. Park, J. Deyst, and J. P. How, "Performance and Lyapunov stability on a nonlinear path-following guidance method," *Journal of Guidance, Control, and Dynamics*, vol. 30, no. 6, pp. 1718–1728, 2007.

[19] D. Nelson, D. Barber, T. McLain, and R. Beard, "Vector field path following for miniature air vehicles," *IEEE Transactions on Robotics*, vol. 23, no. 3, pp. 519–529, 2007.

[20] A. Ratnoo, P. Sujit, and M. Kothari, "Optimal path following for high wind flights," in *18th World Congress of the International Federation of Automatic Control (IFAC)*, Milan, Italy, August 2011.

[21] M. Kothari, I. Postlehwaite, D. Gu, and A. Suboptimal Path, "Planning algorithm using rapidly-exploring random tress," *International Journal of Aerospace Innovations*, vol. 2, no. 1, pp. 93–104, 2010.

[22] P. B. Sujit, S. Saripalli, and J. B. Sousa, "An evolution of UAV path following algorithms," *2013 European Control Conference (ECC)*, 2013, Zurich, Switzerland, July 17-19, 2013, 2013.

[23] C. E. Lin and Y. H. Lai, "Quasi-ADS-B based UAV conflict detection and resolution to manned aircraft," *Journal of Electrical and Computer Engineering*, vol. 2015, Article ID 297859, 12 pages, 2015.